

Effective Hamiltonian for $\text{Ga}_{1-x}\text{Mn}_x\text{As}$ in the Dilute Limit

Gregory A. Fiete^{1,2,3}, Gergely Zarand^{1,2,3} and Kedar Damle^{1,4}

¹Department of Physics, Harvard University, Cambridge MA 02138

²Materials Science Division, Argonne National Laboratory, 9700 South Cass Avenue, Argonne IL, 60429

³Research Institute of Physics, Technical University Budapest, H-1521 Hungary

⁴Department of Physics and Astronomy, Rice University, Houston, TX 77005

We derive an effective Hamiltonian for $\text{Ga}_{1-x}\text{Mn}_x\text{As}$ in the dilute limit, where $\text{Ga}_{1-x}\text{Mn}_x\text{As}$ can be described in terms of spin $F = 3=2$ polarons hopping between the Mn sites and coupled to the local Mn spins. We determine the parameters of our model from microscopic calculations. Our approach treats the extremely large Coulomb interaction in a non-perturbative way, captures the effects of strong spin-orbit coupling and disorder, and is appropriate for other p-doped magnetic semiconductors. Our model applies to uncompensated Mn concentrations up to $x = 0.03$.

Physics numbers: 75.30.Ds, 75.40.Gb, 75.50.Dd

Since the discovery of dilute III-V magnetic semiconductors with relatively high Curie temperatures [1], magnetic semiconductors have become the subject of very intense research [2]. Since the magnetic ions (usually Mn) responsible for the ferromagnetism are dissolved into the semiconductor itself, these materials could provide a unique opportunity to integrate ferromagnetic elements into larger, nonmagnetic, semiconducting devices.

In this paper we focus mostly on one of the most studied magnetic semiconductors, $\text{Ga}_{1-x}\text{Mn}_x\text{As}$, with a maximum Curie temperature $T_c = 110\text{K}$ [1], though most of our calculations carry over to other p-doped III-V magnetic semiconductors [3]. In $\text{Ga}_{1-x}\text{Mn}_x\text{As}$ substitutional Mn²⁺ play a fundamental role: They provide local spin $S = 3=2$ moments, and they also dope holes into the valence band [4]. Since the Mn²⁺ ions are negatively charged compared to Ga³⁺, in the very dilute limit they bind these holes, forming an acceptor level with a binding energy of about $E_b = 112\text{m eV}$ [4]. As the Mn concentration increases, these acceptor states start to overlap and form an impurity band, which for even larger Mn concentrations merges with the valence band. Though the actual concentration at which the impurity band disappears is not known, according to optical conductivity measurements [5], this impurity band seems to persist at least up to nominal Mn concentrations of about $x = 0.05$. ARPES data [6,7] and the fact that even "metallic" samples feature a resistivity upturn at low temperature [8] and seem to be on the localized side of the transition, suggest that for smaller concentrations (and maybe even for relatively large nominal concentrations) one may be able to describe $\text{Ga}_{1-x}\text{Mn}_x\text{As}$ in terms of an impurity band [9].

In $\text{Ga}_{1-x}\text{Mn}_x\text{As}$ the Coulomb potential created by the Mn ions is by far the largest energy scale in the problem [10], but spin-orbit coupling in the hole band is also quite large compared to the exchange coupling between the holes and the Mn spins [4].

Fortunately, in the dilute limit Coulomb scattering on the Mn ions can be handled non-perturbatively. We can

therefore attempt to derive a many-body Hamiltonian in this limit that captures spin-orbit effects, treats the large Coulomb interaction non-perturbatively, and also incorporates the exchange coupling between the local moments and the holes. As we mentioned above, the model we construct is very general and appropriate for describing other p-doped III-V semiconductors as well, and a slightly modified version of it can be used for p-doped II-VI magnetic semiconductors [3].

The top of the valence band in $\text{Ga}_{1-x}\text{Mn}_x\text{As}$ can be described in terms of spin $j = 3=2$ holes [11]. Ignoring for the moment the exchange interaction between the Mn spin and the holes, in the so-called spherical approximation, the motion of the holes in the Coulomb potential of an Mn ion is described by the following Hamiltonian [12],

$$H_0 = \frac{\hbar^2}{2m} \vec{p}^2 - \frac{e^2}{r} + V_{cc}(r); \quad (1)$$

where $m = 7.65$ is a mass renormalization parameter, m is the free electron mass, $\hbar = 0.77$ is the strength of the spin-orbit coupling, $\epsilon_0 = 10$ is the dielectric constant of GaAs, and V_{cc} is the so-called central cell correction [13]. The spin-orbit coupling term in Eq. (1) couples the momentum tensor of the holes $\vec{p} = p_x \hat{x} + p_y \hat{y} + p_z \hat{z}$ to their quadrupole momentum, $J = (j_x j_x + j_y j_y + j_z j_z)/2 = j(j+1)/3$.

The bound states of H_0 (without the central cell correction) have been studied in detail in the seminal paper of Baldereschi and Lipari [12]. Due to the spherical symmetry, the total momentum, $F = \vec{L} + \vec{j}$, is a conserved quantity, where \vec{L} is the orbital angular momentum. The ground state of H_0 is a four-fold degenerate $F = 3=2$ multiplet that contains a substantial d-wave contribution in the case of GaAs due to the strong spin-orbit coupling. In Fig. 1 we illustrate the importance of this d-wave component by presenting the spatial dependence of the hole polarization, $\vec{j}(r)$, for the state $F = 3=2; F_z = 3=2$ which we calculated directly from the Baldereschi-Lipari wave functions with the central cell correction. The direction of the induced hole polarization has a strong angular de-

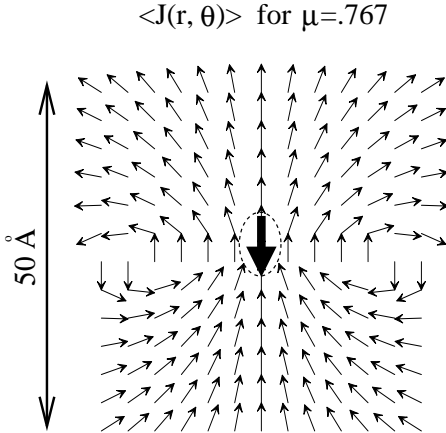


FIG. 1. Polarization of a bound hole in the state $F = 3=2; F_z = 3=2i$ in $\text{Ga}_1-x\text{Mn}_x\text{As}$ around a Mn ion (dark arrow pointing downwards represents the Mn $S = 5/2$ spin). Only the direction of the polarization is indicated. The magnitude falls off on a scale $\sim 10 \text{ \AA}$.

pendence due to the d-wave component.

In the dilute limit, for most purposes, we can restrict ourselves to this fourfold degenerate $F = 3=2$ acceptor level. In the presence of a Mn spin the fourfold degeneracy of the state is lifted due to the exchange interaction between the Mn spin S at the origin:

$$H_{\text{exch}} = G S \cdot F; \quad (2)$$

where the exchange coupling, $G = 5 \text{ meV}$, can directly be determined by infrared spectroscopy [4]. Thus, in this limit, we can think of the charge carriers in $\text{Ga}_1-x\text{Mn}_x\text{As}$ as spin $F = 3=2$ holes hopping between Mn sites and exchange coupled to the localized Mn spins. However, because of the large d-wave component of the Baldereschi-Lipari wave function, we expect the hopping of these carriers to be strongly spin-direction dependent. This expectation is born out by our microscopic calculations below.

To determine the numerical values of the parameters of our model we carried out a variational study of the molecular orbitals for a pair of Mn ions [3,15]. For the case where both the Mn-Mn bond and the quantization axis of F are parallel to the z -axis, F_z is conserved and the spectrum of the lowest lying levels can be fully characterized by the following Hamiltonian:

$$\begin{aligned} H_{\text{Mn-Mn}}^e = & t(R) c_{1i}^{\dagger} c_{2i} + \text{h.c.} \\ & + \sum_{i=1,2}^X K(R) c_{1i}^2 - \frac{5}{4} + E(R) c_{1i}^{\dagger} c_{1i} \\ & + G \sum_{i=1,2}^X S_i \cdot c_{1i}^{\dagger} F \cdot c_{1i} : \end{aligned} \quad (3)$$

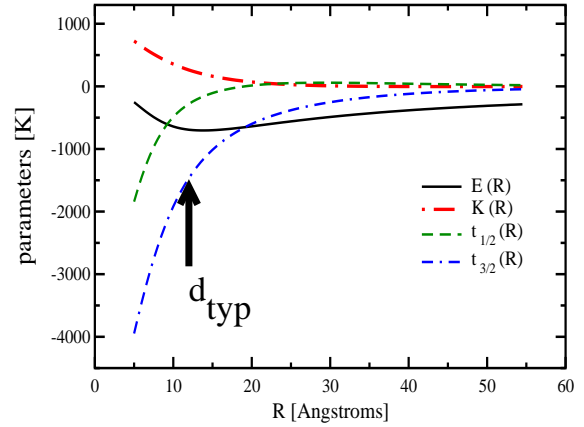


FIG. 2. Parameters of the two-impurity Hamiltonian Eq. (3) obtained from the variational study of two Mn ions. The arrows indicate the typical Mn-Mn distance, d_{typ} , for $x = 0.01$ Mn concentration.

Here c_{ij}^{\dagger} creates a hole at the acceptor level $F = 3=2; F_z = i$ at position i ($i = 1, 2$). By time reversal symmetry, the hopping parameters satisfy $t_{3=2} = t_{3=2}$ and $t_{1=2} = t_{1=2}$. All parameters depend only on the distance R between the two Mn sites. The R -dependence of the four independent couplings is shown in Fig. 2. The most obvious effect of the spin-orbit coupling is that the hoppings $t_{3=2}$ and $t_{1=2}$ substantially differ from each other; Holes that have their spin aligned with the Mn-Mn bond are more mobile.

As indicated by the arrows, at the typical Mn-Mn distance for $x = 0.01$, K and $t_{1=2}$ can be entirely neglected compared to the energy shift E and the hopping $t_{3=2}$. Therefore, in many cases it is enough to keep the latter two terms only in the effective Hamiltonian.

Having determined the effective Hamiltonian for a pair of Mn ions, we can proceed and approximate the Hamiltonian for a given set of positions \mathbf{R} of the Mn ions as:

$$\begin{aligned} H = & \sum_{i,j}^X c_{ij}^{\dagger} t_{ij} c_{ij} + \sum_i^X c_{ij}^{\dagger} (K_i + E_i) c_{ij} \\ & + G \sum_i^X S_i \cdot \sum_j^X F \cdot c_{ij} : \end{aligned} \quad (4)$$

The Hopping matrix t_{ij} above can be obtained by rotating the z -axis along the bond direction \mathbf{r}_{ij} , $t_{ij} = D(\mathbf{r}_{ij}) \hat{t}(R_{ij}) D^{\dagger}(\mathbf{r}_{ij})$, where $D(\mathbf{r}_{ij})$ is a spin 3/2 rotation matrix, and $\hat{t}(R)$ denotes the diagonal matrix $\text{diag } t_{3=2}(R); t_{3=2}(R); t_{1=2}(R); t_{3=2}(R)$. The anisotropy term, K_i , and the energy shift E_i are given by $K_i = \frac{1}{2} \sum_{j \neq i} K(R_{ij}) (\mathbf{r}_{ij} \cdot \mathbf{F})^2 - \frac{5}{4}$ and $E_i = \frac{1}{2} \sum_{j \neq i} E(R_{ij})$, respectively.

So far we have neglected the interaction between holes. In the localized phase, however, this interaction may play an important role. In general, the Coulomb interaction

between holes on different Mn sites has a very complicated form [3], though for large separations the interaction takes on a much simpler form. Fortunately, the dominant interaction term is the on-site hole-hole interaction term. Within the spherical approximation this interaction can be simply expressed as:

$$H_{\text{int}} = \frac{U_N}{2} \sum_i \hat{N}_i^2 + \frac{U_F}{2} \sum_i \hat{F}_i^2; \quad (5)$$

where $\hat{N}_i = \hat{c}_i^\dagger c_i$, $\hat{F}_i = \hat{c}_i^\dagger F c_i$, and $\hat{\cdot} \hat{\cdot} \hat{\cdot}$ denotes normal ordering. We estimated the constants appearing in Eq. (5) by evaluating exchange integrals as $U_N = 2600\text{K}$ and a Hund's rule coupling $U_F = 51\text{K}$.

Eqs. (4) and (5), together with the microscopic parameters of Fig. 2, constitute our central results. They provide a well controlled theoretical framework that is able to capture the most important aspects of dilute magnetic semiconductors such as the localization phase transition, random anisotropy, disorder effects, and frustrated ferromagnetism. Postponing much of our detailed analysis to a longer publication, here we only demonstrate the power of this model on a few examples. Parameters for other materials will be presented elsewhere [3].

To get a better understanding of the model we first computed the ground state of four Mn atoms at a separation of 15\AA due to the interaction mediated by a single hole on the cluster. We treated the Mn spins classically and used the simple mean field approximation of Ref. [9]. We considered only configurations where the Mn ions were positioned on a slightly distorted tetrahedron with three edges of length $a = 15\text{\AA}$ and three edges of length b (see Fig. 3). In all cases, in the ground state, the Mn spins are relatively collinear apart from a slight tilt of the order of $5-10^\circ$. However, the spatial position of the Mn ions generates a strong anisotropy. Thus, the energy depends strongly on the directional orientation of the net spin relative to the underlying lattice. To demonstrate this we calculated the ground state energy as a function of the Mn spin direction (assuming full alignment). For a perfectly regular tetrahedron this anisotropy is rather small, less than 0.5K . However, the anisotropy increases with the ratio b/a , and for $b/a = 1.2$ it can be as large as 20K Mn. In other words, random positions of the Mn ions induce a random anisotropy term that, depending on the disorder, is much larger than the bulk anisotropy, which is of the order of 1K . Thus disorder and spin-orbit coupling together can induce a large random anisotropy energy that can easily be comparable to T_c . These findings are in good agreement with earlier results obtained in the metallic limit [16].

Finally, let us discuss some of the results we obtained for a finite system of $\text{Ga}_x\text{Mn}_x\text{As}$ of linear sizes $L = 10a_{\text{lat}}$ and $L = 13a_{\text{lat}}$ (with $a_{\text{lat}} = 5.65\text{\AA}$, the size of the conventional unit cell) and active Mn concentration $x_{\text{active}} = 0.01$, using the above-described mean field

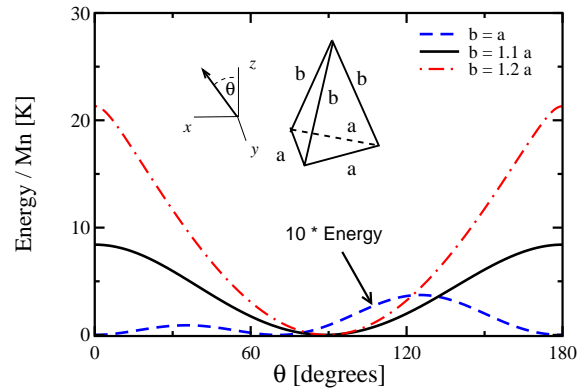


FIG. 3. Anisotropy induced by the distortion of a regular Mn tetrahedron in the presence of a single hole. The Mn-Mn distances are $a = 15\text{\AA}$ and $b = 15\text{\AA}$, $b = 16.5\text{\AA}$, and $b = 18\text{\AA}$, respectively. Note that the distortion generated anisotropy can be almost two orders of magnitude larger than the undistorted anisotropy, which is of the order of about 1K .

techniques at zero temperature. In the calculations presented below, we have not included the effects of Eq. (5). We have to emphasize that x_{active} can be substantially less than the nominal Mn concentration, x , which also includes inactive Mn sites [17], and therefore these calculations may be relevant even for systems with larger nominal Mn concentration. The concentration of holes is also reduced compared to x due to strong compensation effects. In these calculations we assumed that the number of holes is reduced by a factor of $f = 0.3$ compared to the number of Mn ions.

To take into account correlations induced between interstitial Mn ions during the experimental growth process, we introduced a screened Coulomb repulsion between the Mn ions and let them relax for some time t_{relax} using classical $T = 0\text{M}$ onte Carlo simulations. For very large t_{relax} we found that the Mn ions form a regular bcc lattice with some point defects. The data we present here are for intermediate relaxation times, where there is still a lot of disorder in the system.

Once we fixed the Mn positions in a given instance, we solved the mean field equations derived from (4) self-consistently [9]. In our calculations we used periodic boundary conditions and implemented a short distance cut-off in the hopping parameters of Eq. (4) which corresponds to about 8 neighbors for each Mn. The use of this cut-off is justified by the observation that our molecular orbit calculations are only appropriate for "nearest neighbor" ion pairs, and in reality, holes cannot hop directly over the first "shell" of ions. In course of the calculations we started from a configuration with fully aligned classical Mn spins, $\hat{S}_i = S$, and then let the system relax to the nearest metastable state. Similar to the metallic case [16], we find a ferromagnetic state with a largely reduced

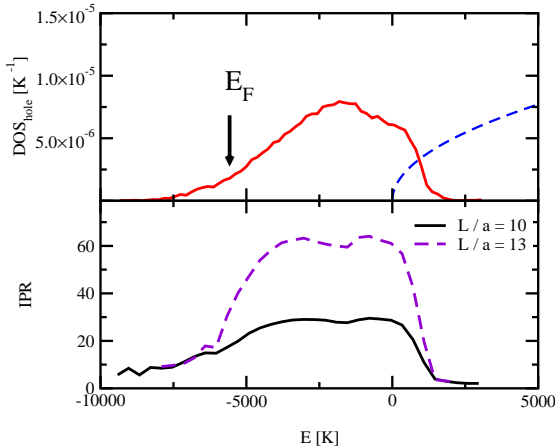


FIG. 4. Top: Computed hole density of states for an $L = 10a$ lattice. We used $x = 0.01$ and $f = 0.3$. For comparison, we also show the density of states of the valence band (dashed line). The Fermi energy is 6500 K. Bottom: The inverse participation ratio for $L = 10a_{\text{lat}}$ and $L = 13a_{\text{lat}}$. States in the tails are localized while states in the middle of the impurity band seem to be delocalized. States in the valence band side tail probably mix with the band and are delocalized in reality.

magnetization, $j \sim 0.4$ for $L = 10a_{\text{lat}}$. We find that this reduction is largely due to spin-orbit coupling, and that the cosine of the angle between the spins and the ground state magnetization has a broad distribution similar to the metallic case [16].

The density of states is shown in Fig. 4 (as a comparison, we also plotted the approximate density of states for the hole band). The halfwidth of the impurity band is about 0.2 eV at this density, which therefore slightly overlaps with the bulk density of states of the holes. However, comparison with the valence hole density of states suggests that at this concentration a well-formed impurity band may still be present, and it might even persist up to higher concentrations. Indeed, as mentioned in the introduction, this scenario seems to be supported by many experiments [7].

The impurity band has a tail of localized states that reaches somewhat inside the band gap. These localized states can be identified by computing the inverse participation ratio, $IPR = \sum_i P_i^2 / P^2$ for various system sizes (see Fig. 4). This tail gradually disappears when we introduce correlations between the Mn ions which tend to form regular structures [3]. In agreement with ARPES data [6], we also find that the chemical potential lies deep (0.5 eV) inside the gap, in the vicinity of the mobility edge, a regime where our model is probably more reliable. This raises the interesting possibility that the localization phase transition in $\text{Ga}_1-x\text{Mn}_x\text{As}$ could happen inside the impurity band and that the fer-

romagnetic phase for smaller Mn concentrations is governed by localized hole states [10,14].

We emphasize that, though our calculations are based on microscopic model calculations, they are certainly only approximate, and more realistic band structure calculations would be needed to give a quantitative answer concerning the role of the impurity band. Also, though the spherical approximation we used is able to reproduce rather well the spectrum of a single acceptor, it might overestimate the effect of spin-orbit coupling.

In summary, based on microscopic calculations we constructed a many-body Hamiltonian that is appropriate for describing $\text{Ga}_1-x\text{Mn}_x\text{As}$ in the dilute limit. We find that the hopping of the carriers is strongly correlated with their spin, $F = 3/2$. This spin-dependent hopping is absolutely crucial for capturing spin-orbit coupling induced random anisotropy terms, the lifetime of the magnon excitations, or even to capture the universality class of the localization phase transition correctly. Our calculations suggest the presence of an impurity band for $x_{\text{active}} = 0.01$ Mn concentration.

We are grateful to B. Janko, M. Berciu, R. Bhattacharya, A. H. MacDonald, P. Schiffer, and especially J.K. Furdyna, X. Liu, and E. Sasaki for stimulating discussions. This research has been supported by the U.S. DOE, Office of Science, NSF Grants No. DMR-9985978 and DMR-97-14725, and Hungarian Grants No. OTKA F030041, T038162, and N 31769.

- [1] H. Ohno, *Science* 281, 951 (1998).
- [2] For recent reviews see J. K. On闲ig et al. in *Electronic Structure and Magnetism of Complex Materials*, edited by D. J. Singh and D. A. Papanastopoulos (Springer Verlag 2002); R. N. Bhatt et al., *J. Superconductivity* 15, 71 (2002); T. Dietl, cond-mat/0201282.
- [3] G. Fiete, G. Zarand and K. Damle (unpublished).
- [4] M. Linnarsson et al., *Phys. Rev. B* 55, 6938 (1997);
- [5] E. J. Singley et al., *Phys. Rev. Lett.* 89, 097203 (2002).
- [6] J. Okabayashi et al., *Phys. Rev. B* 64, 125304 (2001).
- [7] H. Asklund et al., *Phys. Rev. B* 66, 115319 (2002).
- [8] A. Van Esch et al., *Phys. Rev. B* 56, 13103 (1997).
- [9] M. P. Kennett, M. Berciu and R. N. Bhatt, *Phys. Rev. B* 66, 045207 (2002).
- [10] C. Timm, F. Schaefer and F. von Oppen, *Phys. Rev. Lett.* 89, 137201 (2002).
- [11] W. Kohn and J.M. Luttinger, *Phys. Rev.* 98, 915 (1955).
- [12] A. Baldereschi, and N.O. Lipari, *Phys. Rev. B* 8, 2697 (1973).
- [13] A.K. Bhattacharjee and C. Benoit a la Guillaume, *Solid State Comm.* 113, 17 (2000).
- [14] S.-R. Yang and A. H. MacDonald, cond-mat/0202021.
- [15] A.C. Durst, R.N. Bhatt and P.A. Wol, *Phys. Rev. B* 65, 235205 (2002).
- [16] G. Zarand and B. Janko, *Phys. Rev. Lett.* 89, 047201 (2002).
- [17] K.M. Yu, W.W. Slawikiewicz et al., *Appl. Phys. Lett.* 81, 844 (2002), K.M. Yu et al., *Phys. Rev. B* 65, 201303 (2002).